

Available online at www.synsint.com

Synthesis and Sintering

ISSN 2564-0186 (Print), ISSN 2564-0194 (Online)



Research article

Impact of bridging oxygens formation on optical properties of Fe^{3+} doped $\text{Li}_2\text{O}-\text{Al}_2\text{O}_3-\text{SiO}_2-\text{TiO}_2$ glasses



A. Faeghinia

Ceramic Department, Materials and Energy Research Center (MERC), P.O. Box 31779-83634, Karaj, Iran

ABSTRACT

In this study, the structural chemistry of Fe^{3+} doped $\text{Li}_2\text{O}-\text{Al}_2\text{O}_3-\text{SiO}_2-\text{TiO}_2$ (LAST) glasses has been analyzed utilizing UV-Vis spectroscopy. Optical parameters like absorption and extinction coefficients, indirect and direct optical band gaps, Urbach energy as well as Fermi energy level of samples were estimated via their absorption spectra. Then, it was tried to make a relationship between the variation of mentioned parameters and structural chemistry of different doped samples. Results of the investigation illustrated that even a little change in the microstructure of glassy samples has an effect on optical parameters and accordingly it could be sensible. Furthermore, it was revealed that Fe^{3+} ions have the role of network forming in the structure of glass by increasing the formation of bridging oxygens (BOs) in the matrix.

© 2022 The Authors. Published by Synsint Research Group.

KEYWORDS

UV-Vis absorption spectra
Glass
Short-range order
Bridging oxygens formation
Optical parameters
Structural chemistry



1. Introduction

Undoubtedly, progress in materials science will be limited due to the lack of data available on the microstructure of materials. Analysis of materials structure containing long-range order of crystals is a sort of a routine process. Nowadays there is a diversity of techniques which is being utilized for prediction of crystalline structures such as transmission electron microscopy (TEM), X-ray diffractometry (XRD) and so on [1–4]. Nevertheless, extraction of data is still in a serious doubt for the amorphous structures due to the short-range order of crystals distributed stochastically in the bulk of samples. In solid state chemistry, in order to investigate the structural evolution of amorphous materials, spectroscopic methods are used. Hence, various techniques have been proposed based on the interaction of electromagnetic wave (EW) with matter. Accordingly, interaction of EW in each region could be attributed to the resonance or absorption of EW by electrons, atoms, molecules, spin of electrons etc. Each of them could be interpreted for the structural evaluation [5–8].

In advanced technologies, heavy doped materials are utilized for production of the small, high power optical devices [9, 10]. Glassy materials are the interested materials for production of small, high

power devices due to their high solubility of dopants in amorphous matrix. It is almost obvious that introduction of a special dopant into a relatively suitable host could be used for the generation of precise optical and electrical devices. As a dopant, when d outer-shell electrons of transition metals is surrounded by the attraction and repulsion fields, there will be a special ligand field for the dopants which could lead to a special optical or electrical properties in the bulk [11–13]. According to the features of LAS glasses like high transmissibility, near zero thermal expansion and non-linear optical properties, they are utilized in advanced applications. Due to the aforesaid characteristics, LAST glasses are recognized as precision optical apparatuses [14, 15]. In this study, it is attempted to physically analyze the UV-Vis absorption spectrum of LAST glass doped by various amount of Fe_2O_3 , then make a correlation between the physical parameters and structural chemistry of this matter.

2. Experimental procedure

Analytical reagents of Li_2CO_3 , Al_2O_3 , TiO_2 , SiO_2 and Fe_2O_3 (Merck Company, Germany) were selected as the starting materials. Raw materials were thoroughly mixed to prepare about 50 g batch. Then, the

* Corresponding author. E-mail address: a.faeghinia@merc.ac.ir (A. Faeghinia)

Received 25 December 2021; Received in revised form 9 March 2022; Accepted 10 March 2022.

Peer review under responsibility of Synsint Research Group. This is an open access article under the CC BY license (<https://creativecommons.org/licenses/by/4.0/>).
<https://doi.org/10.53063/synsint.2022.2179>

mixed batch melted in alumina crucibles for 120 min at 1400 °C via conventional electrical furnace. The melted batch was poured into a pre-heated stainless steel mold and then allowed to cool down to the ambient temperature. Therefore, the composition of 14.5Li₂O-19.8Al₂O₃-63.7SiO₂-2TiO₂ (wt%) doped with 0 to 1.5 wt% Fe₂O₃ was selected to prepare the glass specimens. ICP analysis (Wuxi Jiebo Electrical Technology Co., Ltd. China) was employed to calculate the solubility of alumina crucibles in the melt, and based on this data, the content of Al₂O₃ in the batch was justified. In order to optical measurements, the glass specimens were cut to the thickness of 1 cm and then were polished to optical quality. A spectrophotometer (T70 UV-VIS PG instruments) was used for optical absorption in the range of UV-Vis spectrum in room temperature. These spectra was utilized to calculate Fermi energy level, extinction and absorption coefficients, Urbach energy, and indirect and direct optical band gaps.

3. Results and discussion

Adding transition metal oxides such as Fe₂O₃ to oxide glasses provides a new ability to enhance features of such materials to use in electronic, electrochemical, and electro-optic applications. Fe can appear as Fe²⁺ and Fe³⁺ in glassy matrix and lead to different developed structural units owing to the presence of various valence its states. Improvement of the chemical stability and durability of these glasses occurs by the addition of Fe₂O₃. Due to broad range of applications of transition metal ions and their influence in modification of the structure, it is very interesting to study in detail the effect of Fe₂O₃ addition on the structural, physical and optical properties of oxide glasses [16–18].

3.1. Spectra of UV-Vis absorption

Absorption spectra of LAST glasses containing 0–1.5% Fe₂O₃ dopant are shown in Fig. 1. Illustrated absorption edge in all glassy samples could be attributed to excitation of electrons in the samples.

These graphs have been divided to three different regions. Each will be discussed in details in the following sections.

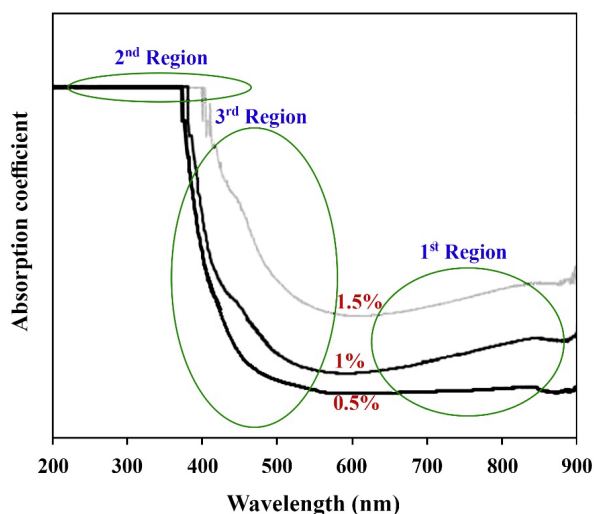


Fig. 1. UV-Vis absorption spectra related to LAST glass doped by different content of Fe₂O₃.

3.2. Calculation of absorption coefficient

In optics, a quantity characterizing how simply a medium or material can be penetrated via a light beam is known as the absorption coefficient [19].

The relative transparency of the medium to the light beam is recognized as a small absorption coefficient and the rapid absorption of a beam by a medium is known as the definition of a large absorption coefficient [20]. Units of reciprocal length are used to measure absorption coefficient.

$$\alpha = \frac{1}{L} \ln \frac{I_0}{I} \quad (1)$$

where α , L , I_0 , and I are absorption coefficient, path length, the intensity of incident beam and intensity of transmitted beam, respectively [21].

It is explainable that optical constants of material, including absorption coefficient (α) and refractive index (n_o), have effect on the electromagnetic waves spreading through sample in which n_o influences on their phase and α affects the amplitude of beam waves. Absorption coefficient of samples was calculated for all range of UV-Vis spectra using Eq. 1.

3.3. Calculation of extinction coefficient

Imaginary section of the refraction complex index related to light absorption is recognized as extinction coefficient of sample that can be determined via Eq. 2:

$$k = \alpha \lambda / 4\pi \quad (2)$$

where k and λ shows extinction coefficient and the wavelength of EW in vacuum condition, respectively [11, 22, 23]. Using Eq. 2 extinction coefficient of each sample was calculated in whole UV-Vis range.

3.4. Direct and indirect band gaps

Based on Tauc's reports [24, 25], there is a relationship between absorption coefficient and band gap energy of a sample.

$$\alpha(\nu) = \beta^2 (h\nu - E_g^{\text{opt}})^n / h\nu \quad (3)$$

where E_g^{opt} shows the optical band gap of glass. $h\nu$ is the incident photon energy that has various values depending on the of incident light frequency that is probing the specimen. n that could be variable amounts 1/3, 1/2, 2, and 3, related to direct forbidden and direct allowed, indirect allowed, and indirect forbidden transitions, respectively. Plotting $(\alpha h\nu)^{1/n}$ versus photon energy ($h\nu$) leads to drawing a direct line. In such cases, dividing intercept by slope equals to energy band gap of optical transitions [26]. β is a constant showing a temperature independent parameter called band tailing factor. It should be noted that this parameter depends on refractive index (n_o) of specimen calculated via:

$$\beta = \sqrt{(4\pi/c)\sigma_0 / n_o \Delta E} \quad (4)$$

where ΔE and σ_0 are the tail width of localized states in the typically forbidden gap and the electrical conductivity at absolute zero [24, 27]. Indirect and Direct optical band gaps of each sample are illustrated in Table 1.

Table 1. Energy states of Fe₂O₃-doped LAST glass.

Sample	E _f	Direct band gap	Indirect band gap	E _U
0% Fe ₂ O ₃	3.94	2.77	3.51	0.41
0.5% Fe ₂ O ₃	3.66	2.53	3.22	0.32
1% Fe ₂ O ₃	3.27	2.46	2.92	0.28
1.5% Fe ₂ O ₃	3.16	2.33	2.56	0.24

3.5. Fermi energy level

Owing to weaker absorption of Visible photons than UV [28,29], extinction coefficient of various glass specimens can be obtained by Fermi-Dirac distribution function as

$$k(\lambda) = \frac{1}{1 + \exp[(E_f - E) / k_B T]} \quad (5)$$

where E_f, E, and K_BT are Fermi energy, the variable energy of sample probe photons and thermal energy resulting from ambient absolute temperature, respectively. E_f can be obtained by fitting the least squares of Eq. 5. Fermi energy of different samples is illustrated in Table 1.

3.6. Urbach energy

Crystallinity degree of material is illustrated by proceeding of absorption coefficient with enhancement of incident beam energy right before absorption edge (3rd Tauc's region). The adsorption coefficient gradually increases with a low slope up to the adsorption edge for samples with disorder microstructure. The slope of this area increases as the degree of crystallinity rises. Eq. 6 can be used to calculate degree of crystallinity,

$$\alpha(v) = \beta \exp(hv / E_U) \quad (6)$$

where E_U is the Urbach energy indicating the width of the band tail of

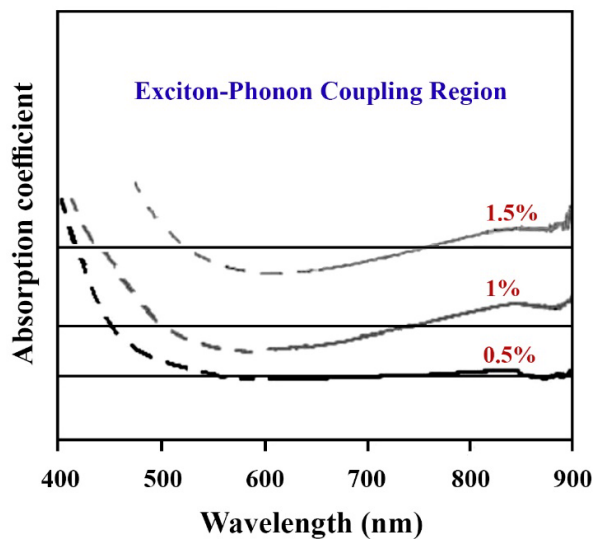


Fig. 2. Exciton-phonon coupling region of spectra of UV-Vis absorption for LAST glass doped by different content of Fe₂O₃.

localized states [20, 26, 29]. Table 1 displays the amount of Urbach energy for various Fe³⁺ doped LAST glasses.

Changing of absorption coefficient with photon energy in many amorphous materials could be discussed in three different regions, according to Tauc [24]:

- Exciton-phonon coupling region
- Interband transition (Tauc's) region
- Urbach region

In the following, it will be tried to discuss more about each section and explain how their changes can be related to structural chemistry of amorphous specimens.

3.7. Exciton-phonon coupling region

The first region in UV-Vis absorption spectrum is recognized by almost constant absorption owing to exciton-phonon coupling. This mentioned area can be seen in the higher visible wavelengths. Fig. 2 shows the exciton-phonon region of spectra of UV-Vis absorption for LAST glass doped by different content of Fe₂O₃ dopant.

As it is obvious, absorption coefficient is more intensive for specimens containing higher amount of Fe₂O₃. In this case, exciton-phonon coupling increases by Fe₂O₃ enhancement. Exciton-phonon coupling will rises by increasing the differences between Fourier transform wave function of electrons and holes in a material. Although this effect is a general property of adding a dopant in a host, its intensive change shows that the selected dopant can change the electronic structure of LAST as well [30]. In the following section, these changes will be discussed in detail.

3.8. Interband transition (Tauc's) region

The second part of UV-Vis absorption spectrum recognized as Tauc region. This region is related to high absorption, which can be employed to calculate optical band gap and is associated with interband transitions. The Tauc's region of LAST glasses doped with different Fe₂O₃ content is shown Fig. 3.

As it is illustrated, absorption edge shifts toward larger wavelengths of electromagnetic wave by increasing the amount of Fe₂O₃ in samples. Accordingly, reduction of band gap and Fermi energy level will be predictable for heavy-doped samples.

In the electronic band structure graphs of materials, the difference of energy (in electron volts) between the bottom of the conduction band and the top of the valence band in insulators and semiconductors generally narrates the band gap.

This band equals to the energy needed to free one electron from the outer shell of its orbit around the nucleus to change to a carrier of the movable charge, and to move freely in the solid. Therefore, an important determinant parameter of electrical conductivity of the material is the band gap. There are several ways to transfer the electrons in solid between energy levels [31]. The electron transition from the bottom valence band to top conduction band stimulated in frequency of absorption edge is the highest energy transition that can be determined by Eq. 7:

$$E_g = hc / \lambda_{ae} \quad (7)$$

where E_g, h, c, and λ_{ae} are the band gap energy, the plank's constant, the speed of light propagating in vacuum, and the wavelength of absorption edge, respectively [26].

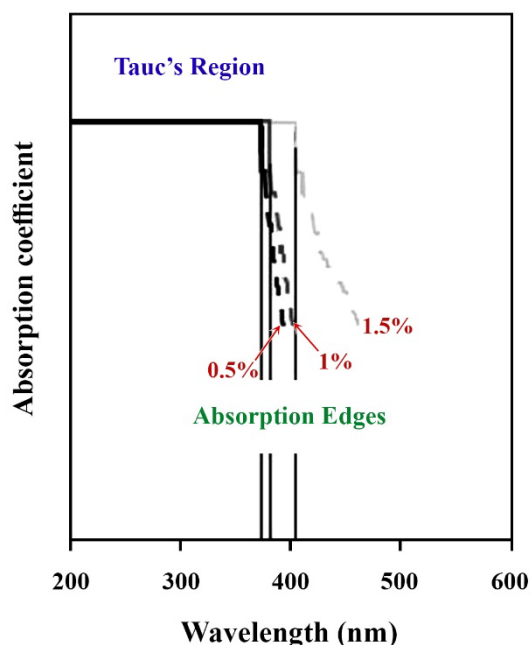


Fig. 3. Tauc's region of spectra of UV-Vis absorption for LAST glass doped by different content of Fe_2O_3 .

According to Table 1, increasing the content of dopant leads to a decrease in indirect and direct optical band gaps. Obviously, introduction of Fe^{3+} ions in the glassy matrix has led to the broadening of conduction band. Al^{3+} ions replace by Fe^{3+} ions. Due to the different ligand field around these ions compared to the other positive ions e.g. Si^{4+} , Al^{3+} and Ti^{4+} , some bands form close to the conduction band. These bands are so close together and the collection of them forms a wide band broadened into the band gap. Hence, band gaps will be reduced. The intensive reduction of indirect band gap of samples by increasing the Fe_2O_3 content (from 3.51 to 3.56) shows the ability of Fe^{3+} ions for giving semiconducting effect to parent glass [32–35].

According to Tauc [24], the decrease in Fermi energy level by enhancement of the Fe_2O_3 content can be attributed to the increase in ionic bonds in the matrix. Compared to the covalent bonds, ionic bonds are increased by introduction of Fe^{3+} ions; hence, Fermi level is fallen to lower energy levels.

3.9. Urbach region

An exponential region in UV-Vis absorption spectrum (The 3rd region) is called Urbach region. This region that lies between Tauc's and exciton-phonon regions is shown for different Fe_2O_3 doped LAST glasses in Fig. 4.

It is reported that many parameters such as electric fields of defects, thermal vibrations, dislocations, and etc. can create tailing of energy states in the forbidden energy gap [36, 37]. Exciton-phonon coupling (dynamic disorder) is the significant item that contributes to edge broadening in crystalline materials. In amorphous ones, existing static disordering results in an additional broadening. Hence, the Urbach energy is resolved in two parts:

$$E_U = E_d + E_{ph} \quad (8)$$

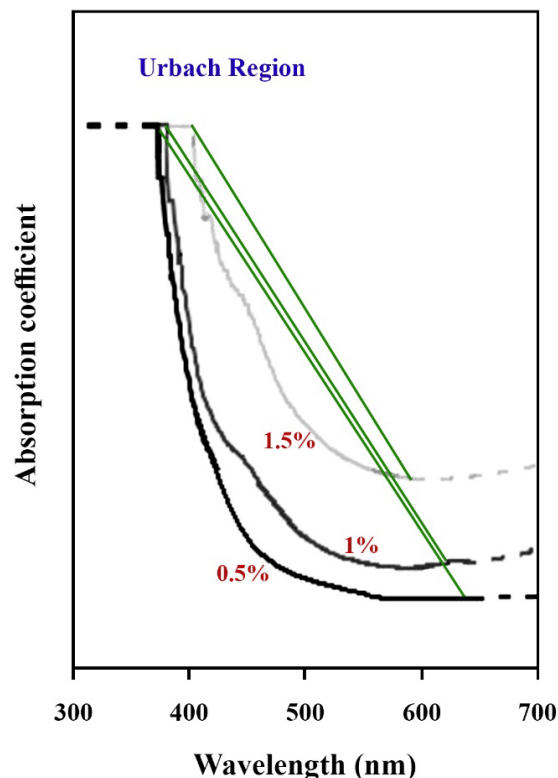


Fig. 4. Urbach region of UV-Vis absorption spectra of LAST glass doped by different content of Fe_2O_3 .

E_{ph} and E_d are related to phonon and disorder-induced broadening. E_d is considered temperature-independent, while E_{ph} depends on temperature according to following relation [38, 39]:

$$E_{ph} = A \coth\left(\frac{B}{2kT}\right) \quad (9)$$

where, A and B are constants that are not temperature dependent. Based on Eq. 8, the zero-level vibrations result in remaining of a non-zero dynamic disorder remains even at low temperatures, but it is almost constant for various doped glassy materials. Therefore, change in Urbach energy significantly can be owing to disorder-induced broadening. Considering the results determined from $\ln(\alpha)$ - $h\nu$ diagrams, increasing the amount of Fe_2O_3 in the sample leads to a decrease in Urbach energy. It means that microstructure of samples will be more ordered by introduction of Fe^{3+} ions in the glassy matrix of LAST. According to reports, this change could be attributed to formation of bridging oxygens (BOs) in the matrix. Tetrahedral chains of SiO_4^{4-} are joined together using O-linkers and the matrix goes toward the crystalline materials [14, 40].

4. Conclusions

Structural chemistry of LAST glass in presence of Fe^{3+} ions was evaluated using the investigation of optical properties of samples calculated from their UV-Vis absorption spectra. Hence, reducing the Urbach energy, Fermi energy level and optical band gaps by enhancement the Fe_2O_3 content in the specimens was ascribed to the

broadening of conduction band owing to the formation of new bands close to the conduction band, increasing ionic bonds in the matrix and formation of more ordered structure owing to the formation of bridging oxygens.

CRediT authorship contribution statement

A. Faeghinia: Conceptualization, Funding acquisition, Investigation, Writing – original draft, Writing – review & editing.

Data availability

The data underlying this article will be shared on reasonable request to the corresponding author.

Declaration of competing interest

The author declares no competing interests.

Funding and acknowledgment

The author gratefully acknowledges the generous financial support provided by the Materials and Energy Research Center, under the Coating Project with Contract No 371398015. This funding played a pivotal role in the successful execution of the research, and the author is sincerely thankful for their contribution to this work.

References

- [1] H. Aghajani, E. Hadavand, N.-S. Peighambaroudost, S. Khameneh-asl, Electro spark deposition of WC–TiC–Co–Ni cermet coatings on St52 steel, *Surf. Interfaces*. 18 (2020) 100392. <https://doi.org/10.1016/j.surf.2019.100392>.
- [2] N. Sadeghi, M.R. Akbarpour, H. Aghajani, A novel two-step mechanical milling approach and in-situ reactive synthesis to fabricate TiC/Graphene layer/Cu nanocomposites and investigation of their mechanical properties, *Mater. Sci. Eng. A*. 734 (2018) 164–170. <https://doi.org/10.1016/j.msea.2018.07.101>.
- [3] N.A. Golnaz, T.T. Arvin, H. Aghajani, Investigation on corrosion behavior of Cu–TiO₂ nanocomposite synthesized by the use of SHS method, *J. Mater. Res. Technol.* 8 (2019) 2216–2222. <https://doi.org/10.1016/j.jmrt.2019.01.025>.
- [4] A. Khan, A. Ali, I. Khan, Sintering behavior and microwave dielectric properties of CaTi_{1-x}(Nb_{1/2}Al_{1/2})_xO₃, *Synth. Sinter*. 1 (2021) 197–201. <https://doi.org/10.53063/synsint.2021.1467>.
- [5] W. Mozgawa, M. Sitarz, M. Król, Spectroscopic characterization of silicate amorphous materials, *Molecular Spectroscopy—Experiment and Theory*, Springer, Cham. (2019) 457–481. https://doi.org/10.1007/978-3-030-01355-4_15.
- [6] A. Ali, Y.W. Chiang, R.M. Santos, X-ray diffraction techniques for mineral characterization: a review for applications, and research directions, *Minerals*. 12 (2022) 205. <https://doi.org/10.3390/min12020205>.
- [7] K.M. Ehrhardt, R.C. Radomsky, S.C. Warren, Quantifying the local structure of nanocrystals, glasses, and interfaces using TEM-based diffraction, *Chem. Mater.* 33 (2021) 8990–9011. <https://doi.org/10.1021/acs.chemmater.1c03017>.
- [8] A.S. Hassanien, I. Sharma, Band-gap engineering, conduction and valence band positions of thermally evaporated amorphous Ge_{15-x}Sb_xSe₅₀Te₃₅ thin films: Influences of Sb upon some optical characterizations and physical parameters, *J. Alloys Compd.* 798 (2019) 750–763. <https://doi.org/10.1016/j.jallcom.2019.05.252>.
- [9] A.S. Abouhaswa, E. Kavaz, A novel B₂O₃–Na₂O–BaO–HgO glass system: synthesis, physical, optical and nuclear shielding features, *Ceram. Int.* 46 (2020) 16166–16177. <https://doi.org/10.1016/j.ceramint.2020.03.172>.
- [10] R. Divina, G. Sathiyapriya, K. Marimuthu, A. Askin, M.I. Sayyed, Structural, elastic, optical and γ-ray shielding behavior of Dy³⁺ ions doped heavy metal incorporated borate glasses, *J. Non. Cryst. Solids*. 545 (2020) 120269. <https://doi.org/10.1016/j.jnoncrysol.2020.120269>.
- [11] A.F.A. El-Rehim, E.A.A. Wahab, M.M.A. Halaka, K.S. Shaaban, Optical properties of SiO₂–TiO₂–La₂O₃–Na₂O–Y₂O₃ glasses and a novel process of preparing the parent glass-ceramics, *Silicon*. 14 (2022) 373–384. <https://doi.org/10.1007/s12633-021-01002-w>.
- [12] R. Lachheb, A. Herrmann, K. Damak, C. Rüssel, R. Maâlej, Optical absorption and photoluminescence properties of chromium in different host glasses, *J. Lumin.* 186 (2017) 152–157. <https://doi.org/10.1016/j.jlumin.2017.02.030>.
- [13] C. Lin, J. Liu, L. Han, H. Gui, J. Song, et al., Study on the structure, thermal and optical properties in Cr₂O₃-incorporated MgO–Al₂O₃–SiO₂–B₂O₃ glass, *J. Non. Cryst. Solids*. 500 (2018) 235–242. <https://doi.org/10.1016/j.jnoncrysol.2018.08.004>.
- [14] M.S. Shakeri, M. Rezvani, Optical properties and structural evaluation of Li₂O–Al₂O₃–SiO₂–TiO₂ glassy semiconductor containing passive agent CeO₂, *Spectrochim. Acta A: Mol. Biomol. Spectrosc.* 83 (2011) 592–597. <https://doi.org/10.1016/j.saa.2011.09.009>.
- [15] A. Arvind, A. Sarkar, V.K. Shrikhande, A.K. Tyagi, G.P. Kothiyal, The effect of TiO₂ addition on the crystallization and phase formation in lithium aluminum silicate (LAS) glasses nucleated by P₂O₅, *J. Phys. Chem. Solids*. 69 (2008) 2622–2627. <https://doi.org/10.1016/j.jpcs.2008.06.003>.
- [16] A. Mekki, D. Holland, K.A. Ziq, C.F. McConville, Structural and magnetic properties of sodium iron germanate glasses, *J. Non. Cryst. Solids*. 272 (2000) 179–190. [https://doi.org/10.1016/S0022-3093\(00\)00235-0](https://doi.org/10.1016/S0022-3093(00)00235-0).
- [17] R. Parmar, R.S. Kundu, R. Punia, P. Aghamkar, N. Kishore, Effect of Fe₂O₃ on the physical and structural properties of bismuth silicate glasses, *AIP Conf. Proc.* (2013) 653–654. <https://doi.org/10.1063/1.4810396>.
- [18] U. Selvaraj, K.J. Rao, Characterization studies of molybdophosphate glasses and a model of structural defects, *J. Non. Cryst. Solids*. 72 (1985) 315–334. [https://doi.org/10.1016/0022-3093\(85\)90187-5](https://doi.org/10.1016/0022-3093(85)90187-5).
- [19] Y. Al-Hadeethi, M.I. Sayyed, Y.S. Rammah, Investigations of the physical, structural, optical and gamma-rays shielding features of B₂O₃–Bi₂O₃–ZnO–CaO glasses, *Ceram. Int.* 45 (2019) 20724–20732. <https://doi.org/10.1016/j.ceramint.2019.07.056>.
- [20] M.S. Shakeri, M. Rezvani, Optical band gap and spectroscopic study of lithium alumino silicate glass containing Y³⁺ ions, *Spectrochim. Acta A. Mol. Biomol. Spectrosc.* 79 (2011) 1920–1925. <https://doi.org/10.1016/j.saa.2011.05.090>.
- [21] T.F. Tadros, *Basic Principles of Dispersions, Handbook of Colloid and Interface Science*, De Gruyter, Berlin, Boston. (2018). <https://doi.org/10.1515/9783110541953>.
- [22] K. Bahedi, M. Addou, A. Mrigal, H. Ftouhi, A. Talbi, et al., A spectroscopic study for determining linear optical and predicting nonlinear optical properties of sprayed ZnO:W thin films: an effect of morphology, *Opt. Rev.* 29 (2022) 25–33. <https://doi.org/10.1007/s10043-021-00718-9>.
- [23] K.S. Shaaban, A.M. Ali, Y.B. Saddeek, K.A. Aly, A. Dahshan, S.A. Amin, Synthesis, mechanical and optical features of Dy₂O₃ doped lead alkali borosilicate glasses, *Silicon*. 11 (2019) 1853–1861. <https://doi.org/10.1007/s12633-018-0004-0>.
- [24] J. Tauc, *Amorphous and Liquid Semiconductors*, Springer, New York, NY. (1974). <https://doi.org/10.1007/978-1-4615-8705-7>.
- [25] A. Kumar, R. Kumar, N. Verma, A.V. Anupama, H.K. Choudhary, et al., Effect of the band gap and the defect states present within band gap on the non-linear optical absorption behaviour of yttrium

- aluminium iron garnets, *Opt. Mater.* 108 (2020) 110163. <https://doi.org/10.1016/j.optmat.2020.110163>.
- [26] F. El-Diasty, F.A. Abdel Wahab, M. Abdel-Baki, Optical band gap studies on lithium aluminum silicate glasses doped with Cr³⁺ ions, *J. Appl. Phys.* 100 (2006) 093511. <https://doi.org/10.1063/1.2362926>.
- [27] N.F. Mott, E.A. Davis, *Electronic processes in non-crystalline materials*, 2nd ed., Oxford University Press, New York. (1979).
- [28] X. Zhang, H. Su, Y. Zhao, T. Tan, Antimicrobial activities of hydrophilic polyurethane/titanium dioxide complex film under visible light irradiation, *J. Photochem. Photobiol. A: Chem.* 199 (2008) 123–129. <https://doi.org/10.1016/j.jphotochem.2008.05.002>.
- [29] V. Khani, P. Alizadeh, M.S. Shakeri, Optical properties of transparent glass–ceramics containing lithium–mica nanocrystals: Crystallization effect, *Mater. Res. Bull.* 48 (2013) 3579–3584. <https://doi.org/10.1016/j.materresbull.2013.05.061>.
- [30] D.M. Sagar, R.R. Cooney, S.L. Sewall, E.A. Dias, M.M. Barsan, et al., Size dependent, state-resolved studies of exciton-phonon couplings in strongly confined semiconductor quantum dots, *Phys. Rev. B.* 77 (2008) 235321. <https://doi.org/10.1103/PhysRevB.77.235321>.
- [31] S.R. Munishwar, P.P. Pawar, S. Ughade, R.S. Gedam, Size dependent effect of electron-hole recombination of CdS quantum dots on emission of Dy³⁺ ions in boro-silicate glasses through energy transfer, *J. Alloys Compd.* 725 (2017) 115–122. <https://doi.org/10.1016/j.jallcom.2017.07.146>.
- [32] A.S. Abouhaswa, Y.S. Rammah, G.M. Turkey, Characterization of zinc lead-borate glasses doped with Fe³⁺ ions: optical, dielectric, and ac-conductivity investigations, *J. Mater. Sci. Mater. Electron.* 31 (2020) 17044–17054. <https://doi.org/10.1007/s10854-020-04262-1>.
- [33] F. Yakuphanoglu, G. Barım, I. Erol, The effect of FeCl₃ on the optical constants and optical band gap of MBZMA-co-MMA polymer thin films, *Phys. B: Condens. Matter.* 391 (2007) 136–140. <https://doi.org/10.1016/j.physb.2006.09.009>.
- [34] P. Pradubkorn, S. Maensiri, E. Swatsitang, P. Laokul, Preparation and characterization of hollow TiO₂ nanospheres: The effect of Fe³⁺ doping on their microstructure and electronic structure, *Curr. Appl. Phys.* 20 (2020) 178–185. <https://doi.org/10.1016/j.cap.2019.11.002>.
- [35] S. Sood, A. Umar, S.K. Mehta, S.K. Kansal, Highly effective Fe-doped TiO₂ nanoparticles photocatalysts for visible-light driven photocatalytic degradation of toxic organic compounds, *J. Colloid Interface Sci.* 450 (2015) 213–223. <https://doi.org/10.1016/j.jcis.2015.03.018>.
- [36] G. Kaur, M. Kumar, A. Arora, O.P. Pandey, K. Singh, Influence of Y₂O₃ on structural and optical properties of SiO₂–BaO–ZnO–x B₂O₃–(10–x) Y₂O₃ glasses and glass ceramics, *J. Non. Cryst. Solids.* 357 (2011) 858–863. <https://doi.org/10.1016/j.jnoncrysol.2010.11.103>.
- [37] G. Kaur, O.P. Pandey, K. Singh, Effect of modifiers field strength on optical, structural and mechanical properties of lanthanum borosilicate glasses, *J. Non. Cryst. Solids.* 358 (2012) 2589–2596. <https://doi.org/10.1016/j.jnoncrysol.2012.06.006>.
- [38] A.A. Ali, M.H. Shaaban, Optical and electrical properties of Nd³⁺ doped TeBiY borate glasses, *Silicon.* 10 (2018) 1503–1511. <https://doi.org/10.1007/s12633-017-9633-y>.
- [39] B. Kressdorf, T. Meyer, M. ten Brink, C. Seick, S. Melles, et al., Orbital-order phase transition in Pr_{1–x}Ca_xMnO₃ probed by photovoltaics, *Phys. Rev. B.* 103 (2021) 235122. <https://doi.org/10.1103/PhysRevB.103.235122>.
- [40] A.C. Hannon, S. Vaishnav, O.L.G. Alderman, P.A. Bingham, The structure of sodium silicate glass from neutron diffraction and modeling of oxygen-oxygen correlations, *J. Am. Ceram. Soc.* 104 (2021) 6155–6171. <https://doi.org/10.1111/jace.17993>.